Moving Beyond Cyanoarene Thermally Activated Delayed Fluorescence Compounds as Photocatalysts: An Assessment of the Performance of a Pyrimidyl Sulfone Photocatalyst in Comparison to 4CzIPN

Megan Amy Bryden,[a] Francis Millward,[a] Tomas Matulaitis,[a] Dongyang Chen,[a] Marco Villa,[b] Andrea Fermi,[b,c] Sultan Cetin,[b] Paola Ceroni [b,c,]* and Eli Zysman-Colman[a,]*

[a]Organic Semiconductor Centre, EaStCHEM School of Chemistry, University of St Andrews, St Andrews, Fife, U.K., KY16 9ST, Fax: +44-1334 463808; Tel: +44-1334 463826;
E-mail: eli.zysman-colman@st-andrews.ac.uk;
URL: http://www.zysman-colman.com
[b]Department of Chemistry Ciamician, University of Bologna, Via Selmi 2, 40126 Bologna, Italy; e-mail: paola.ceroni@unibo.it
[c]Center for Chemical Catalysis–C3, University of Bologna, via Selmi 2, 40126 Bologna, Italy

Abstract

Carbazolyl dicyanobenzene (CDCB) derivates exhibiting thermally activated delayed fluorescence (TADF) have shown themselves to be excellent photocatalysts over recent years, particularly **4CzIPN**, although investigation into organic TADF compounds as photocatalysts outside of the CDCB group has been limited. Herein, we report an alternative donor-acceptor TADF structure, 9,9′-(sulfonylbis(pyrimidine-5,2-diyl))bis(3,6-di-*tert*-butyl-9H-carbazole), **pDTCz-DPmS**, for use as a photocatalyst (PC). A comparison of the electrochemical and photophysical properties of **pDTCz-DPmS** with **4CzIPN** in a range of solvents identifies the former as a better ground state

reducing agent and photoreductant, while both exhibit similar oxidation capabilities in the ground and excited state. The increased conjugation of **pDTCz-DPmS** relative to **4CzIPN** presents a more intense CT band in the UV-Vis absorption spectrum, aiding in the light absorption of this molecule. Prompt and delayed emission lifetimes are observed for **pDTCz-DPmS**, confirming the TADF nature, both of which are significantly long lived to participate in productive photochemistry. These combined properties make **pDTCz-DPmS** useful in photocatalysis reactions, covering a range of photoredox oxidative and reductive quenching reactions, as well as those involving a dual Ni(II) cocatalyst, alongside energy transfer processes. The higher triplet energy and increased photostability of **pDTCz-DPmS** compared with **4CzIPN** were found to be particular advantages of this organic photocatalyst.

Introduction

Over the last two decades, photoredox catalysis has become a widespread and useful tool in organic synthesis.[1–3] This is in part due to the use of much milder reaction conditions in photocatalysis in comparison to the typically higher temperatures and stoichiometric use of reductants, some of which are toxic, often required in traditional thermal synthesis. Additionally, photocatalysis provides alternative and new chemoselectivity, allowing a route to synthons not easily accessible using other synthetic methodologies.[4] As such, photocatalysis has received a resurgence of interest, with just under 17,000 papers published on this topic between 2020 and 2021 combined.[5]

Typically, transition metal complexes based on ruthenium(II) or iridium(III) metals have been the most popular photocatalysts used in homogeneous photocatalysis on account of their well understood and desirable photophysical properties, including their visible-light absorption, long-lived excited states, and versatile redox potentials that can be easily tuned through variation of the ligand field around the metal.[6] However, issues relating to toxicity, natural abundance of these metals and associated cost have motivated the search for alternative photocatalysts, with both Earth-abundant metal complexes[7] and organic compounds[3] identified as potentially viable options for their replacement.

Particularly, since 2016 the organic compound 2,4,5,6-tetra(9*H*-carbazol-9-yl)isophthalonitrile, **4CzIPN**, (Figure **1a**) has become a popular choice as a photocatalyst.[8–10] First developed as an emitter for organic light-emitting diodes (OLEDs),[11] this compound possesses remarkably similar photophysical properties to the commonly used [Ir(dF(CF_3)ppy)$_2$(dtbbpy)]PF_6 [(dF(CF_3)ppy) = 2-(2,4-difluorophenyl)-5-(trifluoromethyl)pyridinato and dtbbpy = 4,4′-di-*tert*-butyl-2,2′-bipyridine] (Figure **1b**).[12,13] **4CzIPN** absorbs into the visible region of the electromagnetic spectrum (λ_{abs} = 435 nm in MeCN),[10] has a long-lived excited state lifetime as it shows thermally activated delayed fluorescence (TADF), (τ_p = 18.7 ns and τ_d = 1390 ns in MeCN,[14] where τ_p and τ_d refer to the prompt and delayed fluorescence lifetimes, respectively), and it possesses a suitable range of redox potentials (Table **1**). **4CzIPN** is composed of an isophthalonitrile acceptor core, decorated with four carbazole electron donor moieties. The steric interactions between adjacent carbazole groups create large torsions between the donor groups to the isophthalonitrile unit. The resultant highly twisted structure ensures that the highest occupied molecular orbital (HOMO) is localized on the donor groups while the lowest unoccupied molecular orbital (LUMO) is located on the acceptor phthalonitrile moiety, leading to a small exchange integral and a correspondingly small singlet-triplet excited state energy gap, ΔE_{ST}. The suitably small ΔE_{ST} is required for the observed TADF associated with this compound.[15]

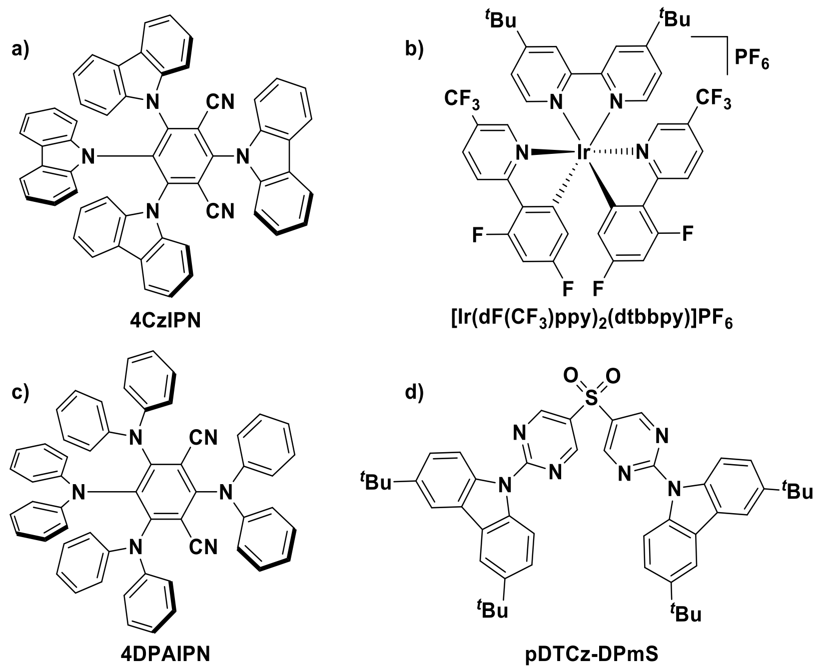

Figure **1**. Structures of a) **4CzIPN**, b) [Ir(dF(CF_3)ppy)$_2$(dtbbpy)]PF_6, c) **4DPAIPN** and d) **pDTCz-DPmS**.

A particular benefit of donor-acceptor organic TADF compounds such as **4CzIPN** lies in the facility to modulate their optoelectronic properties through modification of the structures of the donor or acceptor units, which, due to their relatively small electronic coupling, impact mostly independently the HOMO and LUMO levels, respectively.[16] This facile tuning of the photophysical and electrochemical properties is an attractive and beneficial quality, one that historically has been challenging to achieve with organic photocatalysts.[17] To date, there are now over 200 reports that demonstrate the use of **4CzIPN** and related donor-acceptor compounds, such as **4DPAIPN** (Figure **1c**), as effective photocatalysts.[8,18] Despite the thousands of examples of organic TADF compounds used as emitters in OLEDs,[16] very few of these compounds have been investigated as potential photocatalysts.[8] Recently, imidazoacridine-based TADF compounds were shown to be effective energy transfer photocatalysts in [2+2] cycloadditions.[19] The work of Kwon *et al.*[20] is notable as they explored computationally a wide variety of donor-acceptor architectures as potential photocatalysts in polymerisation reactions. Their study revealed that a selection of donor-acceptor compounds incorporating a sulfone acceptor unit showed useful photocatalytic activity in these reactions.

Inspired by this report, we identified a donor-acceptor sulfone-containing compound, 9,9′-(sulfonylbis(pyrimidine-5,2-diyl))bis(3,6-di-*tert*-butyl-9H-carbazole), **pDTCz-DPmS**, (Figure **1d**), that we had previously developed as a TADF emitter in OLEDs,[21] for use as a potential photocatalyst. This compound possesses a wider ground state redox window, a longer delayed lifetime and is significantly more (photo)reducing than **4CzIPN** (Table **1**).

Table **1**. Selected optoelectronic properties of **4CzIPN** and **pDTCz-DPmS**.[a]

Compound	λ_{abs} / nm	λ_{PL} / nm	$E_{0,0}$ / eV	ΔE_{ST} / eV	τ_p / ns	τ_d / µs	E_{ox} / V	E_{red} / V	E^*_{ox}/ V	E^*_{red}/ V
4CzIPN	448	544	2.60	0.12[b]	24.6[b]	2.04[b]	1.51	-1.21	-1.09	1.39
pDTCz-DPmS	363	524	3.01	0.27	3.0	3.4	1.57	-1.67	-1.44	1.34

[a)] Values are reported in dichloromethane. $E_{0,0}$ determined from the intersection point between the normalized absorption and emission spectra. ΔE_{ST} was calculated as the difference of the first singlet (E_{S1}) and first triplet (E_{T1}) excited state energies ($\Delta E_{ST} = E_{S1} - E_{T1}$), estimated from the onsets of the prompt fluorescence and phosphorescence spectra at 77 K, respectively. τ_p and τ_d refer to the prompt and delayed fluorescence lifetimes, respectively. Redox potentials are reported vs SCE and are obtained from the maxima of the oxidation and reduction waves in the DPV. $E^*_{ox} = E_{ox} - E_{0,0}$ and $E^*_{red} = E_{red} + E_{0,0}$. [b)] Values taken from reference [14] in DCM.

Results and Discussion

Electrochemical and photophysical characterization

The relevant electrochemical and photophysical data of **pDTCz-DPmS** were first ascertained in a range of different polarity solvents to reflect the medium used in the photocatalytic testing (*vide infra*) and these results were cross-compared with density functional theory (DFT) calculations (*vide infra*). The solvents tetrahydrofuran (THF), dichloromethane (DCM), *N*,*N*-dimethylformamide (DMF) and acetonitrile (MeCN) were chosen for investigation due to their frequent use as the medium in photocatalytic reactions.

Cyclic voltammetry (CV) and differential pulse voltammetry (DPV) measurements for **pDTCz-DPmS** and **4CzIPN** permitted the determination of the ground and excited state redox potentials, thermodynamic parameters that are of greatest relevance to photoredox catalysis to assess the feasibility of the single electron transfer (SET) events. Measurements were obtained in THF, DCM, DMF and MeCN; due to poor solubility in MeCN, no measurements were possible in this solvent for **pDTCz-DPmS**. The solvent windows for THF and DMF are limited in the oxidation range, hence the oxidation potentials could not be determined in these solvents.

The CVs of **pDTCz-DPmS** show both chemically irreversible oxidation and reduction waves, while **4CzIPN** exhibits an irreversible oxidation wave and reversible reduction wave in most solvents (Figure **S7**). The redox potentials for both compounds are provided in Table **S2**. While the ground state oxidation potentials in DCM of **4CzIPN** and **pDTCz-DPmS** are similar at 1.51 V and 1.57 V, respectively, the latter compound exhibits a significantly more negative ground state reduction potential (-1.21 V and -1.67 V, respectively, in DCM), implying that **pDTCz-DPmS** will be a more effective ground state reducing agent. Small variations of up to 50 mV in E_{red} are obtained for both compounds as a function of solvent polarity. Generally, with increasing solvent polarity, a more negative E_{red} value is observed. Due the small electrochemical windows of THF and DMF, the impact of solvent polarity on E_{ox} could not be determined.

The UV-Vis absorption spectra of **4CzIPN** and **pDTCz-DPmS** are similar, with both compounds possessing low energy charge transfer (CT) bands (λ_{abs} = 448 nm and 363 nm, respectively, in DCM). Due to the greater conjugation between donor and acceptor in **pDTCz-DPmS**, which is a result of its more planar conformation, these CT bands are much more intense (Figure **2a**). The onset of absorption is significantly more red-shifted in **4CzIPN** in comparison to **pDTCz-DPmS**. There is a limited degree of negative solvatochromic effect observed for both compounds (Figure **S8**), reflecting a decrease in the transition dipole moment of the compounds in the excited state in these solvents.

The normalized steady-state photoluminescence (PL) spectra of **4CzIPN** and **pDTCz-DPmS** in DCM are presented in Figure **2b**. The Gaussian band shape, alongside the observed positive solvatochromism (Figure **S8**), provide evidence of the charge transfer (CT) character of the emissive excited state. The optical gap, $E_{0,0}$, identified from the intersection point between the normalized absorption and emission spectra (Table **S3**) are 2.60 and 3.01 eV for **4CzIPN** and **pDTCz-DPmS**, respectively, in DCM. **pDTCz-DPmS** displays a much larger $E_{0,0}$ than **4CzIPN**, irrespective of solvent. This is due to both the emission of **pDTCz-DPmS** being slightly blue-shifted relative to **4CzIPN** (λ_{PL} = 524 nm and 544 nm in DCM, respectively) as well as the red-shifted CT absorption band present in **4CzIPN** compared to that in **pDTCz-DPmS**. As a result, **pDTCz-DPmS** has an optical gap of *ca.* 0.5 eV larger than that of **4CzIPN**; thus, **pDTCz-DPmS** has a wider excited state redox window (Table **S3**). The excited state reduction potentials are relatively similar, regardless of solvent choice (E^{*}_{red} = 1.34 and 1.39 V for **pDTCz-DPmS** and **4CzIPN** in DCM, respectively), while **pDTCz-DPmS** is a considerably stronger photoreductant than **4CzIPN** (E^{*}_{ox} = -1.44 V and -1.09 V, respectively, in DCM).

The photoluminescence quantum yields, measured in degassed conditions, are strongly dependent on solvent polarity with a value of 42% in toluene and 2.0% in DMF solution (Table **2**). In an attempt to better ascertain trends associated with the solvent polarity, toluene was also employed as a solvent for photophysical measurements since it is nonpolar. The photoluminescence quantum yields measured under air-equilibrated solution correspond roughly to the prompt emission and show a similar trend. The ratio of the prompt and delayed emission quantum yield changes from 2:1 in toluene and DMF to almost 5:1 in THF and DCM, without a clear trend evident with respect to the solvent polarity.

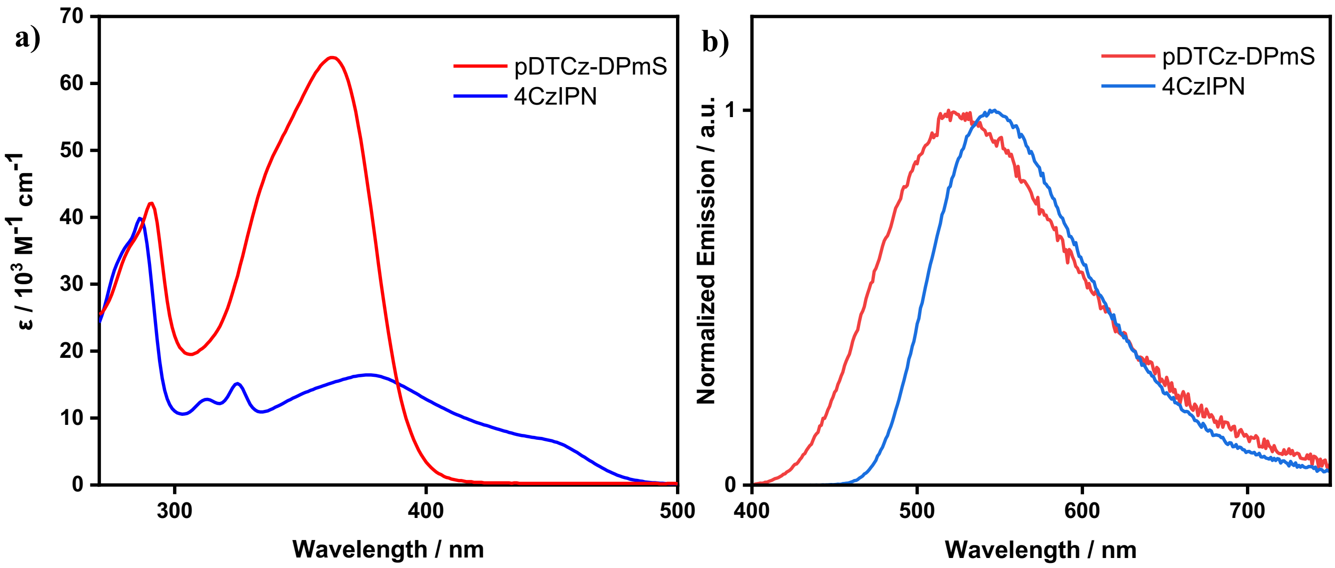

Figure **2**. a) UV-Vis absorption spectra and b) PL spectra for **4CzIPN** and **pDTCz-DPmS** in DCM. λ_{exc} = 420 nm for **4CzIPN** and 360 nm for **pDTCz-DPmS**. Measurements performed at room temperature under air.

The time-resolved PL decays of **pDTCz-DPmS** were measured for 10^{-5} M solutions under vacuum at room temperature (Figure **S9**). In toluene, THF, DCM and DMF, the emission decays with bi-exponential kinetics (Table **2**). The prompt emission occurs with a 3 to 7 ns lifetime (τ_p) in all four solvents, while the microsecond-range delayed emission lifetime, τ_d, becomes shorter with increasing solvent polarity. Regardless of solvent, the excited states of both compounds are sufficiently long-lived to participate in photocatalysis. The faster TADF decay can be linked to the larger reverse intersystem crossing (RISC) rate and is indicative of a smaller ΔE_{ST} (0.12 eV and 0.27 eV for **4CzIPN** and **pDTCz-DPmS**, respectively, in DCM).

For **4CzIPN**, Adachi *et al.* found that with increasing solvent polarity, k_{ISC} between S_1 to T_1 decreases (from 5.1×10^7 s^{-1} in toluene to 2.2×10^6 s^{-1} in MeCN).[14] This was hypothesised to be a result of the interaction between the singlet excited state of **4CzIPN** and solvent molecules, which suppressed k_{ISC} as has been seen in carbene and fluorenone systems.[22,23] Indeed, Wang *et al*. suggested that in the carbene system, the solvated carbene must first be desolvated before ISC can occur, thus causing the k_{ISC} to decrease. This trend in k_{ISC} was proposed to be the reason behind the decrease in the photoluminescence quantum yield (Φ_{PL}) in more polar solvents (94% and 18% for toluene and MeCN, respectively). By contrast, the value of k_{RISC} was found to increase with solvent polarity (from 2.7×10^6 s^{-1} in toluene to 1.4×10^7 s^{-1} in MeCN). These findings are similarly reflected in the trends observed for **pDTCz-DPmS** (Table **2**).

Table **2**. Selected photophysical properties for **pDTCz-DPmS** in toluene, THF, DCM and DMF.[a]

Solvent	Toluene	THF	DCM	DMF
Φ_{PL} / %	42 (28)	17 (14)	7.0 (5.8)	2.0 (1.4)
$\Phi_{PROMPT}/\Phi_{TADF}$	2.0	4.7	4.8	2.3
k_{ISC} / s^{-1} [b]	6.36×10^7	1.78×10^8	1.17×10^8	3.12×10^7
k_{RISC} / s^{-1} [b]	1.39×10^5	2.65×10^5	4.53×10^5	5.19×10^5
τ_p / ns (weighting / %)	7.3 (54)	3 (59)	3 (68)	4 (89)
τ_d / µs (weighting / %)	13.4 (46)	8.1 (41)	3.4 (32)	2.2 (11)
E_{S1} / eV	3.20	3.09	3.20	3.13
E_{T1} / eV	2.95	2.93	2.93	2.97
ΔE_{ST} / eV	0.25	0.16	0.27	0.16

[a] Photoluminescence quantum yields, Φ_{PL}, were determined under deaerated conditions while the values in parentheses refer to the air-equilibrated solutions. Prompt and delayed lifetimes (τ_p and τ_d, respectively) were recorded at room temperature under vacuum using λ_{exc} = 378 nm. The first excited singlet (E_{S1}) and triplet energies (E_{T1}) were determined by the onset of the room temperature photoluminescence and 77 K

phosphorescence spectra, respectively. [b] Rates are determined using the method and assumptions outlined in reference [24].

Photocatalysis investigations

The potential of **pDTCz-DPmS** to act as a photocatalyst was subsequently evaluated in a range of prototypical photochemical reactions that cover the suite of commonly encountered mechanisms: reductive quenching, oxidative quenching, energy transfer and dual metallaphotocatalysis with a Ni(II) co-catalyst (Figure **3**). The performance of **pDTCz-DPmS** was cross-compared with that of **4CzIPN** as well as the reference photocatalysts previously reported for these reactions.

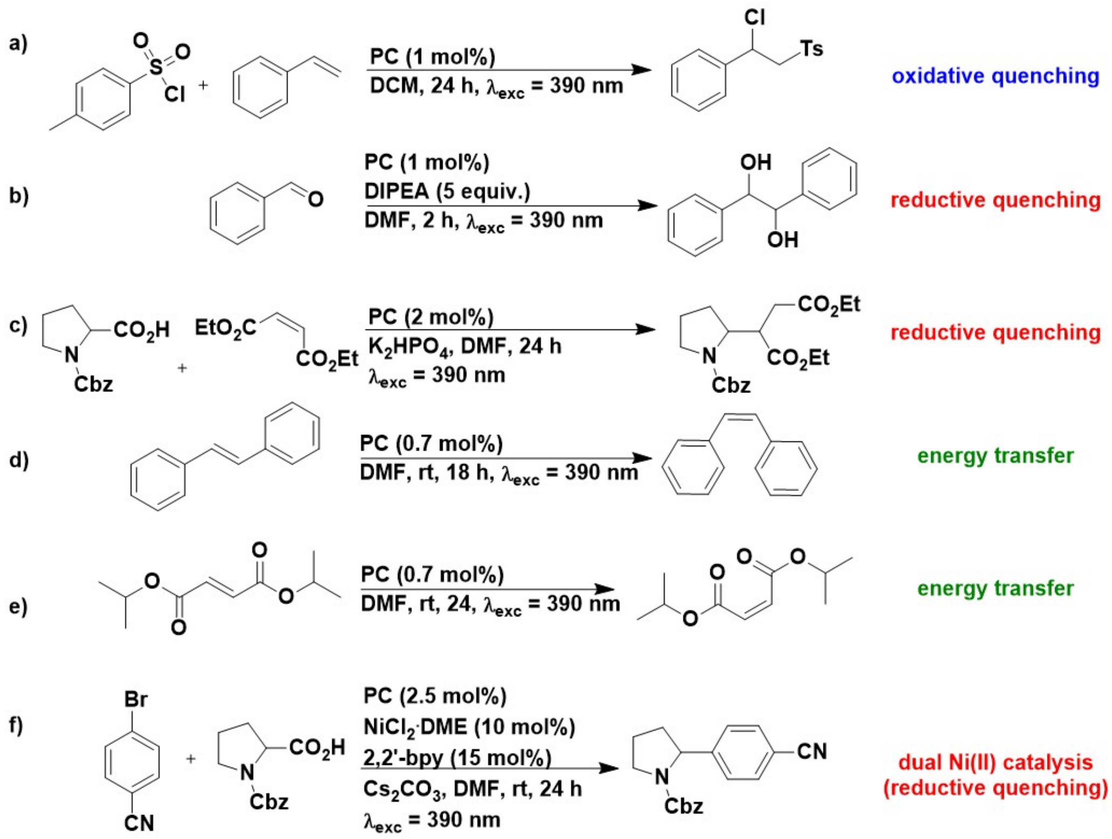

Figure **3**. Photocatalysis reactions investigated: a) oxidative quenching, b) and c) reductive quenching, d) and e) energy transfer and f) dual metallaphotocatalysis with a Ni(II) co-catalyst.

Oxidative quenching

We first assessed the potential of **pDTCz-DPmS** as a photocatalyst in an atom transfer radical addition (ATRA) reaction with styrene and tosyl chloride (TsCl).[25,26] Reiser *et al.* had employed transition metal PCs such as $[Cu(dap)_2]Cl$ or $[Ru(bpy)_3](PF_6)_2$ as the PC, affording under the optimized conditions 96% or 80% of the coupled product, respectively, for the substrates shown in Figure **3a**.[27] The proposed mechanism involves an oxidative quench of the excited PC by TsCl, generating a tosyl radical and a halide anion. The tosyl radical is then proposed to add to the olefin, with the resultant radical being oxidized by the oxidized photocatalyst, closing the photocatalytic cycle. The PC must be sufficiently photoreducing to reduce TsCl (E_{red} = -0.94 V vs SCE)[27] while being capable in its oxidized form to oxidize the carbon-centred radical intermediate. For the copper PCs, the proposed mechanism also involved coordination of the substrates to the metal centre, hence for simplicity, $[Ru(bpy)_3](PF_6)_2$ was used as the reference PC for comparison as $[Cu(dap)_2]Cl$ may be implicated in both inner sphere and outer sphere electron transfer chemistry.

The literature yield of $[Ru(bpy)_3](PF_6)_2$ obtained by Reiser *et al.* using 455 nm CREE XP LEDs as the light source and MeCN as the solvent for 24 h could be replicated using our photocatalytic setup (80% vs 81%, respectively) when matching the conditions as closely as possible, with the use of a 456 nm Kessil lamp being the only significant change. However, these conditions needed to be altered to 390 nm irradiation in DCM due to the absorption profile and solubility of **pDTCz-DPmS**. Under these conditions, the yield obtained from $[Ru(bpy)_3](PF_6)_2$ dropped to 64%. Based on the redox potentials (Table **3**), we envisaged that both **4CzIPN** and **pDTCz-DPmS** could promote this transformation, particularly the latter. Unfortunately, while both could photocatalyze the reaction, they do so in poor yields of 10 and 16%, respectively, with a considerable amount of unreacted styrene detected in the reaction mixture by ^{1}H NMR spectroscopy. It is unclear at this point why the organic TADF photocatalysts perform so much more poorly than $[Ru(bpy)_3](PF_6)_2$.

Table **3**. Average ^{1}H NMR yields obtained in the ATRA reaction and relevant redox potentials of the photocatalysts.[a]

Photocatalyst	E_{ox} / V	E^*_{ox} / V	^{1}H NMR yield / %
$[Ru(bpy)_3](PF_6)_2$	1.42	-0.86	64 ± 3 (80)[b]
4CzIPN	1.51	-1.09	10 ± 1
pDTCz-DPmS	1.57	-1.44	16 ± 2

[a] Redox potentials reported vs SCE and in DCM unless otherwise noted. Values in parentheses indicate the ^{1}H NMR yield obtained in the literature. Reaction conditions followed are those shown in Figure **3** (refer to SI for further details). [b] Value taken from reference [27] using 455 nm irradiation and MeCN as the solvent.

Reductive quenching

We next assessed **pDTCz-DPmS** as a photocatalyst in two reductive quenching reactions: the pinacol coupling of benzaldehyde (Figure **3b**); as well as the decarboxylative addition of *N*-Cbz-Pro to diethyl maleate (Figure **3c**). In the former, the proposed mechanism involves reductive quenching of the PC by di*iso*propylethylamine (DIPEA), followed by reduction of benzaldehyde by the reduced PC, facilitated by the presence of the Lewis acidic radical cation of DIPEA.[28] The iridium PC, $[Ir(ppy)_2(dtbbpy)]PF_6$, provided a reported yield of 44% under the conditions of Rueping *et al.* involving 11 W 450 nm LEDs with MeCN as the solvent for 15 hours, which is matched using our set-up (Table **4**) utilising 390 nm Kessil lamps, DMF as the solvent and a reaction time of only two hours.

Pleasingly, **pDTCz-DPmS** photocatalyzed this reaction but again, despite ostensibly having a larger thermodynamically driving force, the NMR yield falls short of that obtained for **4CzIPN** (Table **4**) when conducting the reaction for a period of two hours. This may be linked to the molar absorptivity, ε, of the two photocatalysts at 390 nm, of which the ε for **4CzIPN** is higher (14.9×10^3 M^{-1} cm^{-1} vs 12.8×10^3 M^{-1} cm^{-1}, for **4CzIPN** and **pDTCz-DPmS**, respectively, see Figure **2a**). Since ε is linked to the rate of reaction,[29] the low yield may be explained by slower reaction kinetics; note that the reaction time is only two hours, following the conditions of Wenger *et al.*[30] Increasing the reaction time to 24 h resulted in a much larger reaction yield for **pDTCz-DPmS** whereas there was only a minor difference in yield when **4CzIPN** was used as the PC (Table **4**), resulting in comparable yields for the two PCs. Under our conditions, the reaction was also found to proceed without the need for a photocatalyst, this is termed the background reaction. Although the background reaction does also increase with the longer time period (Table **S5**), this cannot fully account for the increase in yield for **pDTCz-DPmS**. Notably, PCs such as $[Ru(bpy)_3](PF_6)_2$ cannot turn over this transformation as documented in the literature[28,30] and reproduced with our set-up.

The decarboxylative addition of *N*-Cbz-Pro to diethyl maleate (Figure **3c**) was selected as a model reaction to investigate oxidative photocatalysis through a reductive quenching cycle; both $[Ir(dF(CF_3)ppy)_2(dtbbpy)]PF_6$ and **4CzIPN** have been shown to be highly effective and both of them were described to be reductively quenched by the deprotonated form of *N*-Cbz-Pro.[17,31] According to these literature reports, the PC must be capable of first oxidizing the *N*-Cbz-Pro carboxylate (E_{ox} = 0.68 V vs SCE in DMF for *tert*-butylammonium *N*-Cbz-Pro salt, Figure **S18**) as well as being suitably reducing in the ground state to reduce the *in-situ* generated α-acyl radical, as depicted in Scheme **1**. The literature yield of 93% obtained using $[Ir(dF(CF_3)ppy)_2(dtbbpy)]PF_6$ could be replicated in our setup (Table **4**), while with **4CzIPN** as the PC, the yield obtained was higher than that reported by Zeitler *et al.* (99% vs 80%, respectively).

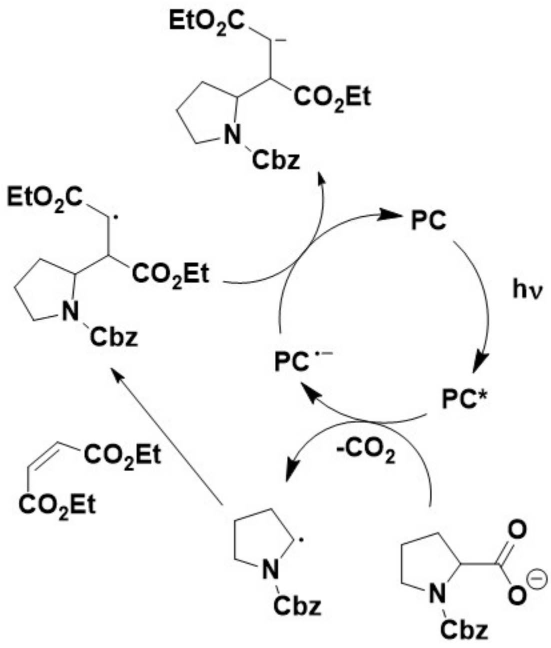

Scheme **1**. Literature reported proposed mechanism for the decarboxylative addition of *N*-Cbz-Pro to diethyl maleate.[1]

pDTCz-DPmS could also photocatalyze this reaction but at a lower yield of 64% (Table **4**). We investigated the mechanism of the photoreaction to provide insight into the origin of the differences in yields compared to the previously reported photocatalysts. We did not observe any quenching of the prompt fluorescence upon addition of the reagents. To our surprise, we observed a strong quenching of the delayed fluorescence of **pDTCz-DPmS** in degassed DMF solution upon addition of diethyl maleate (k_q = 7.0 x 10^8 M^{-1} s^{-1}, Figure **S13**). Upon addition of *N*-Cbz-Pro, quenching was observed only in the presence of K_2HPO_4 and only after a few hours stirring (due to the limited solubility of the base in DMF). The efficiency of quenching of **pDTCz-DPmS** was evaluated at the same concentrations used in the reaction conditions for diethyl maleate and *N*-Cbz-Pro (in the presence of K_2HPO_4): 85% of the excited states are deactivated by diethyl maleate quenching, 8% by *N*-Cbz-Pro quenching and 7% decays by intramolecular processes (see SI form more details). In comparison, for **4CzIPN** quenching is observed only for *N*-Cbz-Pro in the presence of K_2HPO_4 and only after a few hours stirring (Figure **S14**). No quenching is observed after addition of diethyl maleate.

Based on the reduction potential of diethyl maleate (E_{red} = -1.43 V vs SCE in DMF, Figure **S19**), oxidative quenching of **pDTCz-DPmS** (E^{*}_{ox} = -1.44 V vs SCE in DCM) by diethyl maleate is thermodynamically feasible, while this is not the case for **4CzIPN** (E^{*}_{ox} = -1.09 V vs SCE in DCM). To ensure the quenching of **pDTCz-DPmS** by diethyl maleate was occurring through SET, and not by energy transfer via a *Z* → *E* isomerisation process, the irradiation of diethyl maleate in the presence of **pDTCz-DPmS** was conducted. As expected from the reported triplet energies of the maleate and fumarate isomers (E_T = 3.08 eV and 2.87 eV, respectively),[2] **pDTCz-DPmS** (E_T = 2.97 in DMF) could not isomerize diethyl maleate (see SI for more details), therefore we can confidently conclude that this quenching process proceeds via SET.

Combining these experimental observations prompted us to propose an alternative (Scheme **2**) and competitive mechanism to that outlined in Scheme **1**.

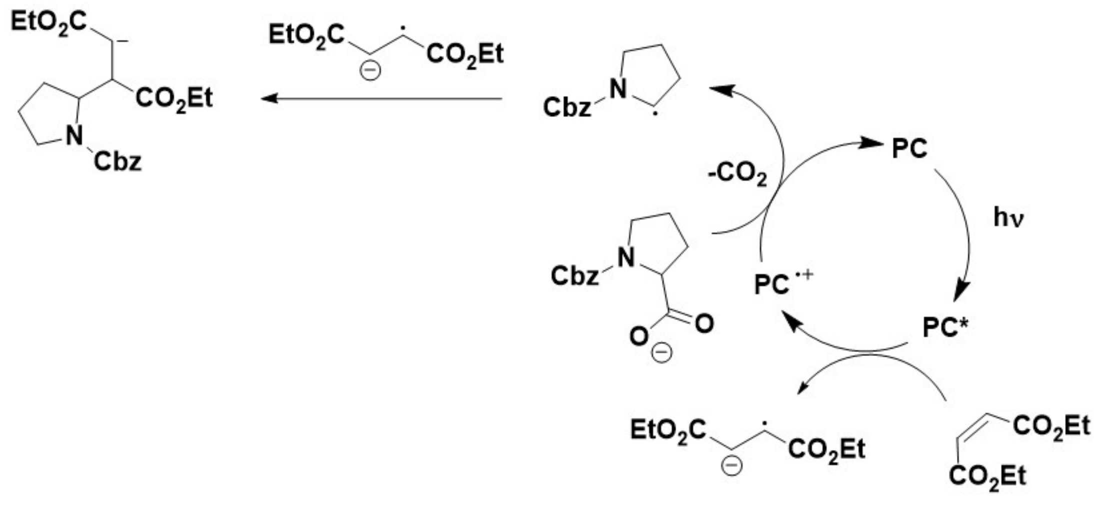

Scheme **2.** Proposed reaction mechanism for the decarboxylative addition of diethyl maleate to *N*-Cbz-Pro when using **pDTCz-DPmS** as a photocatalyst based on our experimental observations.

We also contend that photosubstitution of **4CzIPN** under the reaction conditions may additionally play a role in the yields obtained. Indeed, König *et al*. have recently reported that dicyanobenzene-based PCs undergo photosubstitution of one of the cyano groups when irradiated in the presence of carboxylic acids and base.[32] The resultant photosubstituted product is significantly more photoreducing, in part based on the larger $E_{0,0}$ evidenced by the blue shift of the absorption spectrum. Based on this report, we assessed the photostability of **4CzIPN** and **pDTCz-DPmS** in the presence of *N*-Cbz-Pro and base (Figures **S15** and **S16**), which revealed the photosubstitution of **4CzIPN** while **pDTCz-DPmS** is photostable. The photosubstitution experiment was repeated under the exact reaction conditions, namely in presence of a radical trap in the form of diethyl maleate. Again, the photosubstitution of **4CzIPN** was observed, while **pDTCz-DPmS** remained photostable (Figure **S17** and **S18**).

Table **4**. Average ^{1}H NMR yields obtained for the reductive quenching reactions and relevant redox potentials of the photocatalysts.[a]

Photocatalyst	E_{red} / V	E^*_{red} / V	Reaction	^{1}H NMR yield / %
$[Ir(ppy)_2(dtbbpy)]PF_6$	-1.42	1.08	Pinacol coupling	43 ± 3 74 ± 3[b] (44)[c]
4CzIPN	-1.24	1.40	Pinacol coupling	68 ± 0 76 ± 3[b]
pDTCz-DPmS	-1.62	1.48	Pinacol coupling	32 ± 1 80 ± 3[b]
$[Ir(dF(CF_3)ppy)_2(dtbbpy)]PF_6$	-1.27	1.46	Decarboxylative addition	99 ± 0 (93)[d]
4CzIPN	-1.24	1.40	Decarboxylative addition	99 ± 0 (80)[e]
pDTCz-DPmS	-1.62	1.48	Decarboxylative addition	64 ± 3

[a] Redox potentials reported vs SCE and in DMF unless otherwise noted. Values in parentheses indicate the ^{1}H NMR yield obtained in literature unless otherwise noted. Yields for the pinacol reaction refer to combined yield of the meso:dl isomers. Reaction conditions followed are those shown in Figure **3** unless otherwise noted (refer to SI for further details). [b] Reaction run for 24 h. [c] Value taken from reference [28] using MeCN as the solvent, 2 equiv. NBu_3 (in replacement of DIPEA) and 450 nm irradiation for 15 h. [d] Value taken from reference [31] using 26 W CFL and is an isolated yield using dimethyl maleate as the substrate. [e] Value taken from reference [17] using 455 nm LEDs in MeCN and is an isolated yield.

Energy transfer

Having demonstrated the potential of **pDTCz-DPmS** as a photoredox catalyst in reactions that proceed by both oxidative and reductive quenching mechanisms, we next explored this compound in the context of an energy transfer photocatalytic reaction. We first investigated the *E/Z* isomerization of stilbene (Figure **3d**), following the conditions employed by Zhang *et al.*[33] Reaction yields are shown in Table **5**. The photocatalytic isomerization of alkenes is a well-documented process[34–36] that proceeds via a Dexter energy transfer mechanism. For Dexter energy transfer to be operational, there must be orbital overlap between the donor and acceptor, which can be achieved through bimolecular collisions in an intermolecular reaction. Additionally, spectral overlap between the emission of the energy donor (the photocatalyst) and absorption of the energy acceptor (the *E*-alkene) is required. Triplet energy levels of the PC and the substrate are typically used to crudely assess whether the energy transfer is thermodynamically feasible. To prevent photocatalyzed isomerization of the *Z*-alkene back to the *E*-alkene, the triplet state of the PC must be of intermediate energy to those of the configurational isomers. For stilbene, the E_T are 2.2 eV and 2.5 eV, respectively, for the *E* and *Z* isomers.[37] In the photocatalyzed isomerisation, the *E*-isomer can be selectively photoexcited to its triplet state, forming a triplet diradical intermediate that is then free to rotate to form the thermodynamically less stable *Z*-isomer.

When using *E*-stilbene as the substrate, **pDTCz-DPmS** successfully forms the isomeric product, although only does so in moderate yield of 63% while for **4CzIPN**, the yield of the *Z* isomer is higher at 87%. This is a result of **4CzIPN** possessing a more suitable E_T to sensitize the *E*-isomer while the E_T for **pDTCz-DPmS** is considerably higher, and thus there is a lack of chemoselectivity to selectively sensitize only the *E*-isomer. By contrast, when exploring the *E/Z* isomerization of di*iso*propyl fumarate (Figure **3e**), a higher triplet energy alkene (E_T = 2.7 eV and 3.1 eV, respectively, for the *E* and *Z* isomers),[38] **pDTCz-DPmS** provides a significantly greater yield than **4CzIPN** (81% and 6%, respectively), as well as outperforming the literature photocatalyst $[Ir(dF(CF_3)ppy)_2(dtbbpy)]PF_6$ (58%). In this example, a higher photocatalyst E_T level is required to efficiently sensitize the substrate, which **pDTCz-DPmS** can provide, while **4CzIPN** cannot. The *E*/*Z* directionality of the di*iso*propyl fumarate isomerisation process is facilitated by the stabilising $n_O \rightarrow \pi_{C=O}^*$ interaction of the *Z*-isomer, which reduces the conjugation of the product chromophore and raises the triplet energy of the maleate isomer.[39]

Table **5**. Average ^{1}H NMR yields obtained in the *E*/*Z* isomerization reaction and triplet energy level of the photocatalysts.[a]

Photocatalyst	E_T / eV	Alkene	^{1}H NMR yield / %
$[Ru(bpy)_3](PF_6)_2$	2.13 [e]	*E*-stilbene	81 ± 1 (87) [d]
$[Ir(dF(CF_3)ppy)_2(dtbbpy)]PF_6$	2.65 [c]	di*iso*propyl fumarate	58 ± 1 (88:12) [b, d]
4CzIPN	2.59 [f]	*E*-stilbene	87 ± 1 (6.69) [b, d]
		di*iso*propyl fumarate	6 ± 1 (0:100) [b, d]
pDTCz-DPmS	2.97	*E*-stilbene	63 ± 4
		di*iso*propyl fumarate	81 ± 2

[a] Triplet energy level reported in DMF and obtained at 77 K unless otherwise noted. Values in parentheses indicate the ^{1}H NMR yield obtained in the literature. Reaction conditions followed are those shown in Figure **3** (refer to SI for further details). [b] *Z:E* or *Z/E* ratio. [c] Value taken from reference [40] and was determined in MeCN from the emission maximum. [d] Values taken from reference [33] using a 26 W CFL as the irradiation source. [e] Value taken from reference [41] and determined in an ethanol:methanol (4:1 v/v) glass at 77 K. [f] Value taken from reference [42] and was determined in 2-methyltetrahydrofuran at 77 K.

Dual catalysis with a Ni(II) co-catalyst

Finally, we investigated the potential of **pDTCz-DPmS** in a commonly used Ni-cocatalyzed metallaphotocatalysis reaction involving the cross-coupling of carboxylic acids with aryl halides (Figure **3f**).[10] The proposed mechanism involves the reductive quenching of the excited PC by the carboxylate to yield an alkyl radical following decarboxylation. Closure of the photocatalytic cycle occurs by SET from the reduced PC to the Ni(I) species. Additionally, the PC is proposed to be responsible for the *in situ* generation of the active Ni(0) species through two SET reductions ($E_{red}(Ni^{II}/Ni^{0})$ = -1.2 V vs SCE in DMF).[43] As a result, the PC must be moderately photooxidizing as well as sufficiently reducing in the ground state.

pDTCz-DPmS afforded the coupled product in a yield of 72%, although this is lower than the quantitative 99% yield obtained with **4CzIPN** (Table **6**). Zhang *et al.* also found that despite having appropriate redox potentials, some donor-acceptor PCs failed to perform as well as **4CzIPN**, which they tentatively attributed to their inferior photochemical stability under the reaction conditions.[3] We suspect this is again linked to a combination of the photosubstitution of **4CzIPN** (in contrast to the photostability of **pDTCz-DPmS**) as shown in Figures **S15-18**, as well as the possibility of an alternative oxidative quenching mechanism being in operation, as previously discussed for reaction **3c**.

Table **6**. Average ^{1}H NMR yields obtained in the dual catalysis reaction and relevant redox potentials of the photocatalysts.[a]

Photocatalyst	E_{red} / V	E^{*}_{red} / V	^{1}H NMR yield / %
4CzIPN	-1.24	1.40	99 ± 1 (82) [b]
pDTCz-DPmS	-1.62	1.48	72 ± 4

[a] Redox potentials reported vs SCE in DMF unless otherwise noted. Values in parentheses indicate the isolated yield obtained in the literature. Reaction conditions followed are those shown in Figure **3** (refer to SI for further details). [b] Value taken from

reference [10] using *N*-Boc-Pro irradiated by a 26 W CFL for 10 hours and is an isolated yield.

Conclusions

We have identified a donor-acceptor TADF compound that can perform competitively in a range of photocatalytic reactions with the commonly used **4CzIPN**, encompassing a variety of different mechanisms. In particular, the high triplet energy of **pDTCz-DPmS** permitted the selective and efficient *E/Z* isomerization of high triplet energy substrates. The much-improved photostability of **pDTCz-DPmS** relative to **4CzIPN** under the reaction conditions investigated presents an additional advantage of this compound. As such, our study shows that TADF donor-acceptor compounds beyond **4CzIPN** and the CDCB family can not only be employed but can perform even more efficiently than this popular organic photocatalyst.

Acknowledgements

We are grateful to the University of St Andrews, Syngenta, the EPSRC Centre for Doctoral Training in Critical Resource Catalysis (CRITICAT) for financial support [Ph.D. studentship to "M.B."; Grant code: EP/L016419/1]. We thank Umicore AG for the gift of materials. EZ-C is a Royal Society Leverhulme Trust Senior Research fellow (SRF\R1\201089). E.Z.-C., S.C. and P.C. acknowledge the European Union H2020 research and innovation program under the Marie Skłodowska Curie Grant Agreement (PhotoReAct, No 956324).

Supporting Information

Electronic supplementary information available: synthetic procedures, NMR spectra, electrochemistry, details of DFT calculations (including coordinates of optimised structures), luminescence studies, and photocatalysis set-up.

References

1 G. E. M. Crisenza and P. Melchiorre, *Nature Communications*, 2020, **11**, 803–806.

2 R. C. McAtee, E. J. McClain and C. R. J. Stephenson, *Trends in Chemistry*, 2019, **1**, 111–125.

3 N. A. Romero and D. A. Nicewicz, *Chemical Reviews*, 2016, 10075–10166.

4 T. Noel and E. Zysman-Colman, *Chemical Catalysis*, 2022, 10.1016/j.checat.2021.12.015.

5 SciFinder search on the topic of “photocatalysis” https://scifinder.cas.org/scifinder/view/scifinder/scifinderExplore.jsf (accessed January 2022).

6 C. K. Prier, D. A. Rankic and D. W. C. MacMillan, *Chemical Reviews*, 2013, **113**, 5322–5363.

7 N. Robertson, B. M. Hockin, C. Li and E. Zysman-Colman, *Catalysis Science and Technology*, 2019, **9**, 889–915.

8 M. A. Bryden and E. Zysman-Colman, *Chemical Society Reviews*, 2021, **50**, 7587–7680.

9 T. Shang, L. Lu, Z. Cao, Y. Liu, W. He and B. Yu, *Chemical Communications*, 2019, **55**, 5408–5419.

10 J. Luo and J. Zhang, *ACS Catalysis*, 2016, **6**, 873–877.

11 H. Uoyama, K. Goushi, K. Shizu, H. Nomura and C. Adachi, *Nature*, 2012, **492**, 234–238.

12 M. S. Lowry, J. I. Goldsmith, J. D. Slinker, R. Rohl, R. A. Pascal, G. G. Malliaras and S. Bernhard, *Chemical Materials*, 2005, **17**, 5712–5719.

13 K. Teegardin, J. I. Day, J. Chan and J. Weaver, *Organic Process Research and Development*, 2016, **20**, 1156–1163.

14 R. Ishimatsu, S. Matsunami, K. Shizu, C. Adachi, K. Nakano and T. Imato, *Journal of Physical Chemistry A*, 2013, **117**, 5607–5612.

15 T. J. Penfold, F. B. Dias and A. P. Monkman, *Chemical Communications*, 2018, **54**, 3926–3935.

16 M. Y. Wong and E. Zysman-Colman, *Advanced Materials*, 2017, **29**, 1605444.

17 E. Speckmeier, T. G. Fischer and K. Zeitler, *Journal of the American Chemical Society*, 2018, **140**, 15353–15365.

18 P. P. Singh and V. Srivastava, *Organic & Biomolecular Chemistry*, 2021, 10.1039/d0ob01884h.

19 E. Sauve, D. Mayder, S. Kamal, M. S. Oderinde and Z. Hudson, *Chemical Science*, DOI:10.1039/D1SC05098B.

20 V. K. Singh, C. Yu, S. Badgujar, Y. Kim, Y. Kwon, D. Kim, J. Lee, T. Akhter, G. Thangavel, L. S. Park, J. Lee, P. C. Nandajan, R. Wannemacher, B. Milián-Medina, L. Lüer, K. S. Kim, J. Gierschner and M. S. Kwon, *Nature Catalysis*, 2018, **1**, 794–804.

21 P. L. Dos Santos, D. Chen, P. Rajamalli, T. Matulaitis, D. B. Cordes, A. M. Z. Slawin, D. Jacquemin, E. Zysman-Colman and I. D. W. Samuel, *ACS Applied Materials and Interfaces*, 2019, **11**, 45171–45179.

22 J. Wang, J. Kubicki, H. Peng and M. S. Platz, *Journal of the American Chemical Society*, 2008, **130**, 6604–6609.

23 L. Biczok, T. Berces and F. Marta, *Journal of Physical Chemistry*, 1993, **97**, 8895–8899.

24 F. B. Dias, J. Santos, D. R. Graves, P. Data, R. S. Nobuyasu, M. A. Fox, A. S. Batsanov, T. Palmeira, M. N. Berberan-Santos, M. R. Bryce and A. P. Monkman, *Advanced Science*, 2016, **3**, 1600080.

25 T. Pintauer and K. Matyjaszewski, *Chemical Society Reviews*, 2008, **37**, 1087–1097.

26 E. Arceo, E. Montroni and P. Melchiorre, *Angewandte Chemie International Edition*, 2014, **53**, 12064–12068.

27 A. Hossain, S. Engl, E. Lutsker and O. Reiser, *ACS Catalysis*, 2019, **9**, 1103–1109.

28 M. Nakajima, E. Fava, S. Loescher, Z. Jiang and M. Rueping, *Angewandte Chemie International Edition*, 2015, **54**, 8828–8832.

29 K. C. Harper, E. G. Moschetta, S. V Bordawekar and S. J. Wittenberger, *ACS Central Science*, 2019, **5**, 109–115.

30 L. Schmid, C. Kerzig, A. Prescimone and O. S. Wenger, *JACS Au*, 2021, **1**, 819–832.

31 L. Chu, C. Ohta, Z. Zuo and D. W. C. MacMillan, *Journal of the American Chemical Society*, 2014, **136**, 10886–10889.

32 S. Grotjahn and B. König, *Organic Letters*, 2021, 10.1021/acs.orglett.1c00836.

33 J. Lu, B. Pattengale, Q. Liu, S. Yang, W. Shi, S. Li, J. Huang and J. Zhang, *Journal of the American Chemical Society*, 2018, **140**, 13719–13725.

34 W. Cai, H. Fan, D. Ding, Y. Zhang and W. Wang, *Chemical Communications*, 2017, **53**, 12918–12921.

35 J. B. Metternich, D. G. Artiukhin, M. C. Holland, M. Von Bremen-Kuhne, J. Neugebauer and R. Gilmour, *Journal of Organic Chemistry*, 2017, **82**, 9955–9977.

36 D. C. Fabry, M. A. Ronge and M. Rueping, *Chemistry European Journal*, 2015, **21**, 5350–5354.

37 W. G. Herkstroeter and D. S. McClure, *Journal of the American Chemical Society*, 1968, **90**, 4522–4527.

38 G. S. Hammond, J. Saltiel, A. A. Lamola, N. J. Turro, J. S. Bradshaw, D. O. Cowan, R. C. Counsell, V. Vogt and C. Dalton, *Journal of the American Chemical Society*, 1964, **86**, 3197–3217.

39 T. Neveselý, J. J. Molloy, C. McLaughlin, L. Brüss, C. G. Daniliuc and R. Gilmour, *Angewandte Chemie International Edition*, 2022, **61**, e202113600.

40 A. Singh, K. Teegardin, M. Kelly, K. S. Prasad, S. Krishnan and J. D. Weaver, *Journal of Organometallic Chemistry*, 2015, **776**, 51–59.

41 J. N. Demas and A. W. Adamson, *Journal of the American Chemical Society*, 1971, **93**, 1800–1801.

42 A. Kretzschmar, C. Patze, S. T. Schwaebel and U. H. F. Bunz, *Journal of Organic Chemistry*, 2015, **80**, 9126–9131.

43 J. A. Terrett, J. D. Cuthbertson, V. W. Shurtleff and D. W. C. MacMillan, *Nature*, 2015, **524**, 330–334.

TOC graphic:

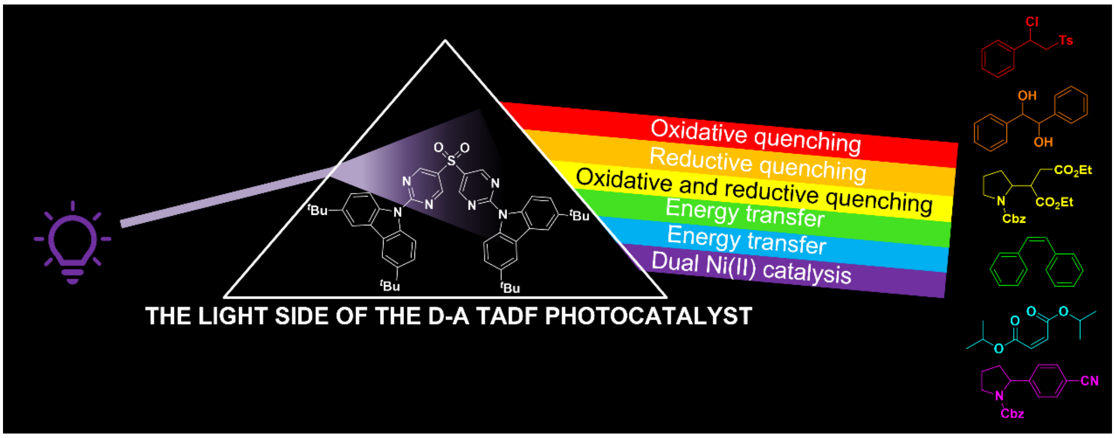

Oxidative quenching
Reductive quenching
Oxidative and reductive quenching
Energy transfer
Energy transfer
Dual Ni(II) catalysis
THE LIGHT SIDE OF THE D-A TADF PHOTOCATALYST